ISSN 1561-8323 (Print)
ISSN 2524-2431 (Online)

ИНФОРМАТИКА

INFORMATICS

UDC 004.932.2 Received 26.07.2026
https://doi.org/10.29235/1561-8323-2026-70-4-286-295 Поступило в редакцию 26.07.2026

Xianyi Wu[1], Guoyan Wang[2], Academician Sergey V. Ablameyko[1], BingYan Liu[3]

[1]Belarusian State University, Minsk, Republic of Belarus
4, Nezavisimosti Ave., 220030, Minsk, Republic of Belarus
[2]National Key Laboratory on ATR, National University of Defense Technology,
People's Republic of China
137, Yanwachi Str., Changsha, Hunan, 410073, China
[3]Joongbu University, Republic of Korea
201, Daehak-ro, Chubumyeon, Geumsan-gun, Chungcheongnam-do, 32713, Republic of Korea

SPIKEYOLO-BOOST: A SPIKING NEURAL NETWORK FOR REMOTE SENSING OBJECT DETECTION BASED ON AN ATTENTION MECHANISM

Abstract. Traditional convolutional neural networks suffer from excessive energy consumption, which restricts their edge deployment for object detection in remote sensing images. Brain-inspired spiking neural networks (SNNs) offer biological plausibility and low-power advantages. At present, the performance of SNNs on object detection tasks still trails behind mainstream models, particularly in complex remote sensing scenes characterized by large-scale variations, cluttered backgrounds, and dense small objects. In this paper, we aim to improve the performance of SNNs for object detection in remote sensing images. We propose the SpikeYOLO-Boost framework. First, we design the SpikeBoT3 spiking hybrid backbone module, which establishes a dual-path global modeling mechanism in the spike domain. Then, we design the SpikeSEAttention spiking channel attention mechanism, which leverages temporal average pooling to achieve channel-wise enhancement in the spike domain, thereby improving feature fusion and robustness.

Keywords: spiking neural networks; remote sensing image object detection; attention mechanism; feature fusion

For citation. Xianyi Wu, Guoyan Wang, Ablameyko S. V., BingYan Liu. SpikeYOLO-Boost: a spiking neural network for remote sensing object detection based on an attention mechanism. *Doklady Natsional'noi akademii nauk Belarusi = Doklady of the National Academy of Sciences of Belarus*, 2026, vol. 70, no. 4, pp. 286–295. https://doi.org/10.29235/1561-8323-2026-70-4-286-295

Xianyi Wu[1], Guoyan Wang[2], академик С. В. Абламейко[1], BingYan Liu[3]

[1]Белорусский государственный университет, Минск, Республика Беларусь
пр-т Независимости, 4, 220030, Минск, Республика Беларусь
[2]Национальная ключевая лаборатория по ATR, Национальный университет оборонных технологий,
Китайская Народная Республика
137, Yanwachi Str., Changsha, Hunan, 410073, China
[3]Университет Чжунбу, Республика Корея
201, Daehak-ro, Chubumyeon, Geumsan-gun, Chungcheongnam-do, 32713,
Republic of Korea

SPIKEYOLO-BOOST: ИМПУЛЬСНАЯ НЕЙРОННАЯ СЕТЬ ДЛЯ ОБНАРУЖЕНИЯ ОБЪЕКТОВ НА ИЗОБРАЖЕНИЯХ ДИСТАНЦИОННОГО ЗОНДИРОВАНИЯ ЗЕМЛИ НА ОСНОВЕ МЕХАНИЗМА ВНИМАНИЯ

Аннотация. Традиционные сверточные нейронные сети отличаются чрезмерным энергопотреблением, что ограничивает их развертывание на периферийных устройствах для обнаружения объектов на изображениях дистанционного зондирования Земли. Нейроморфные импульсные нейронные сети (ИНС) обладают биологической правдоподобностью и низким энергопотреблением, вместе с тем их производительность в задачах обнаружения объектов все еще уступает основным моделям, особенно в сложных сценах дистанционного зондирования, характеризующихся большим разнообразием масштабов, зашумленным фоном и плотно расположенными мелкими объектами. Предлагаются подходы повышения эффективности ИНС для обнаружения объектов на изображениях дистанционного зондирования, а также новая модель SpikeYOLO-Boost. Во-первых, разработан гибридный импульсный модуль SpikeBoT3, формирующий двухпутевой механизм глобального моделирования в импульсной области. Во-вторых, предложен импульсный механизм канального внимания SpikeSEAttention, использующий временное усреднение для усиления канальных признаков в импульсной области, что повышает качество слияния признаков и робастность модели.

Ключевые слова: импульсные нейронные сети, обнаружение объектов на снимках ДЗЗ, механизм внимания, слияние признаков

Для цитирования. SpikeYOLO-Boost: импульсная нейронная сеть для обнаружения объектов на изображениях дистанционного зондирования земли на основе механизма внимания / Xianyi Wu, Guoyan Wang, С. В. Абламейко, BingYan Liu // Доклады Национальной академии наук Беларуси. – 2026. – Т. 70, № 4. – С. 286–295. https://doi.org/10.29235/1561-8323-2026-70-4-286-295

1. Introduction. With the rapid growth in the number of remote sensing satellites, remote sensing technology has become a core component of infrastructure in fields including urban planning, military reconnaissance, environmental monitoring, and disaster early warning [1]. Deep learning, with its capabilities in automatic feature extraction and complex pattern recognition, has become the mainstream technology in the remote sensing field [2]. However, deep learning relies on energy-intensive continuous numerical computation. In the face of massive remote sensing data, the constrained computing and storage resources of on-orbit satellites and airborne platforms [3] pose a severe challenge to real-time processing [4]. Currently, remote sensing object detection mainly depends on powerful ground-based processors. Yet, the limited bandwidth of satellite-to-ground data links means that the time from satellite imaging to completing object detection (e. g., for aircraft) is excessively long and fails to meet practical application demands [3].

Spiking neural networks (SNNs) transmit information via discrete, event-driven spikes, combining low power consumption with high parallelism – traits well-matched to remote sensing edge tasks. Their built-in temporal dynamics capture long-range dependencies, while sparse firing suppresses background clutter and amplifies weak signals from small objects. Yet real-world remote sensing imagery spans wide swaths, varying viewpoints, and large scale disparities. Current SNN detectors still lag on such imagery. They fail to model long-range dependencies among scattered targets, leaving global context underused; their multi-scale fusion lacks channel-level enhancement, so small-object features drown in background noise across deep layers.

These problems severely restrict the further development and engineering application of SNNs in remote sensing. To address these limitations, this paper proposes the SpikeYOLO-Boost enhanced spiking object detection framework.

2. SpikeYOLO-Boost. In 2025, SpikeYOLO [5] replaced conventional binary spikes with an integer-output training strategy, suppressing membrane potential quantization errors and spike degradation. By streamlining YOLO modules and incorporating Meta-SNN blocks, it mitigated gradient instability in deeper networks and enabled end-to-end training. Empirically, its mAP and training accuracy outperformed directly trained SNNs such as EMS-YOLO, while the virtual time-step design reduced inference latency and energy consumption. However, the model still struggled to model long-range dependencies among spatially dispersed targets in complex remote sensing scenes [6], and the absence of a channel attention mechanism during feature fusion weakened its discrimination of multi-scale and small objects.

We build SpikeYOLO-Boost (Fig. 1) on top of SpikeYOLO by inserting SpikeBoT3 at the backbone tail to capture long-range dependencies, and SpikeSEAttention after the neck to reweight channels during multi-scale fusion. This hybrid attention design keeps SNN sparsity and low power, yet pushes accuracy closer to advanced ANNs and extends spiking models to complex remote sensing scenes.

2.1. SpikeMHSA. Multi-Head Self-Attention (MHSA) [7] underpins Transformer-based long-range dependency modeling. We port this mechanism into the spike domain as SpikeMHSA; its architecture is detailed in Fig. 2.

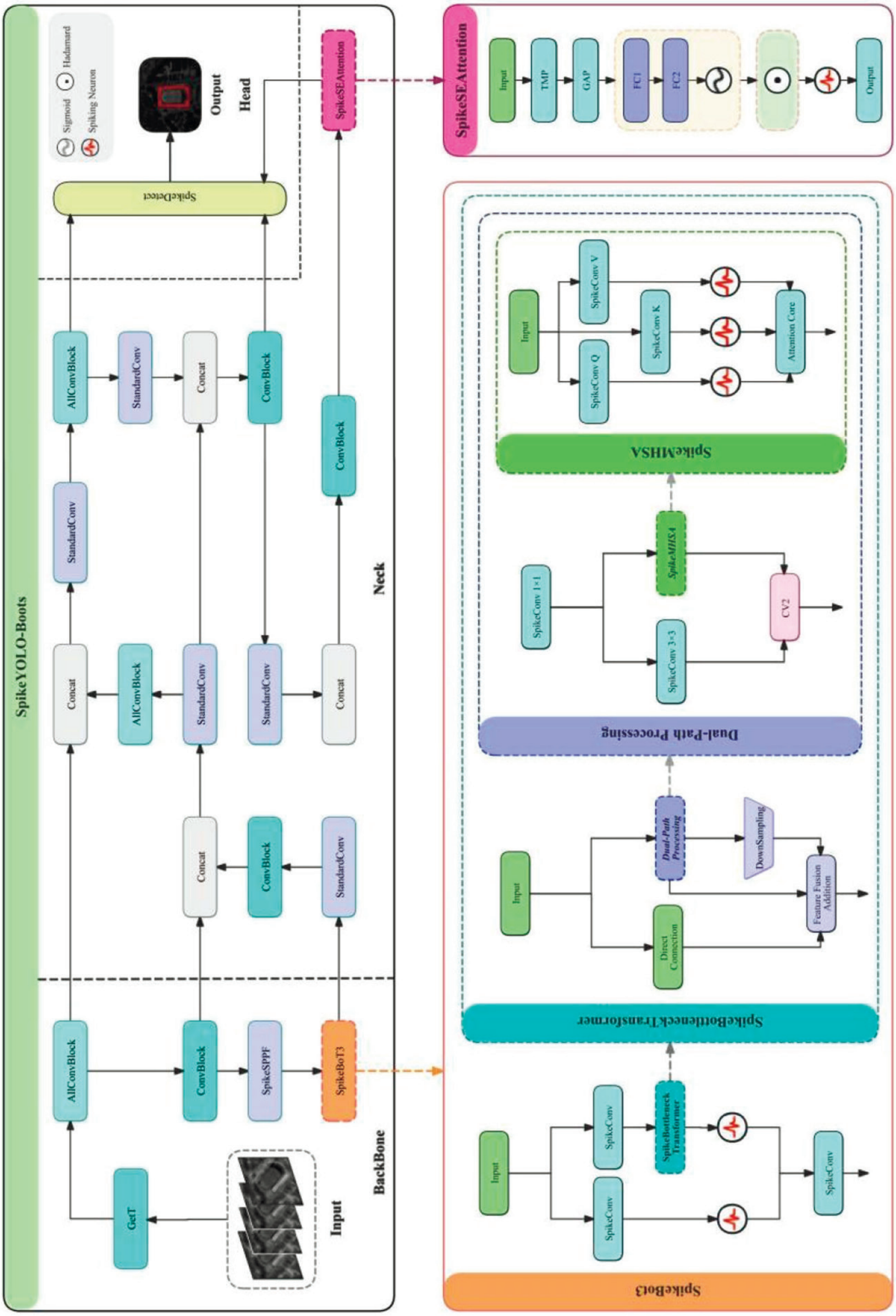

Fig. 1. Architecture of SpikeYOLO-Boost

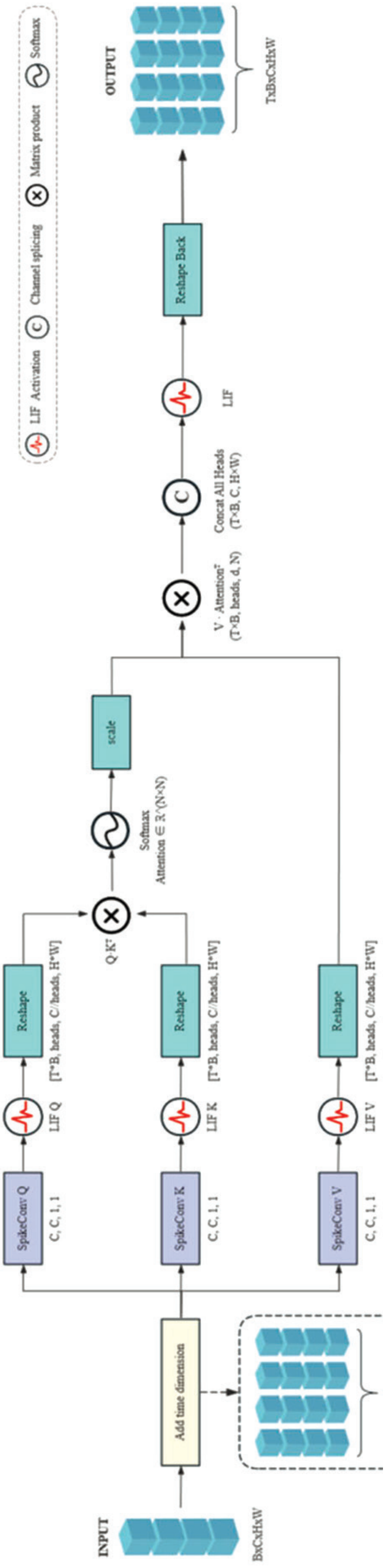

Fig. 2. Structure of SpikeMHSA

First, the input is projected through three independent SpikeConv (1 × 1 convolution) branches to generate the Query (Q), Key (K), and Value (V), with the LIF spiking activation function applied to ensure they retain the event-driven nature:

$$\begin{aligned} Q &= \mathrm{SpikeConv}^{Q}_{1\times1}(\bar{x}) \\ K &= \mathrm{SpikeConv}^{K}_{1\times1}(\bar{x}) \in R^{B\times C\times H\times W}. \\ V &= \mathrm{SpikeConv}^{V}_{1\times1}(\bar{x}) \end{aligned}$$

Subsequently, to enable parallel computation, Q, K, and V are reshaped into a multi-head format [$T \times B$, heads, C/heads, N] (with flattened spatial size $N = H \times W$), where T, B, C, and heads denote the number of time steps, the batch size, the number of channels, and the number of attention heads, respectively.

The similarity matrix $A = QKT$ is computed in the spike domain. It is then scaled by $A \leftarrow A / \sqrt{d_k}$, where $\sqrt{d_k}$ is the dimension of the key vectors, to prevent excessively large values that may lead to vanishing gradients. The scaled similarity is normalized via the softmax function and used to weight the spiking V:

$$\mathrm{Attention}(Q, K, V) = \mathrm{Softmax}\left(\frac{QK^T}{\sqrt{d_k}}\right)V.$$

All head outputs are concatenated along channels and reshaped to the input spatiotemporal size. A final LIF neuron restores the spike representation while preserving the original dimensions. The design thus embeds multi-head attention in SNNs without breaking spike sparsity or temporal dynamics.

2.2. SpikeBottleneckTransformer swaps continuous operations for spike-driven ones – SpikeConv handles convolution, SpikeMHSA replaces standard self-attention, and LIF neurons sit at key junctions (Fig. 3).

A 1 × 1 SpikeConv first squeezes the channel count to form the bottleneck. Features then enter a configurable branch: SpikeMHSA runs global attention when active, otherwise a 3 × 3 SpikeConv covers local receptive fields. The branch output is added back to the residual stream as raw spike sequences, keeping temporal dynamics intact in [T, B, C, H, W] format from input to output.

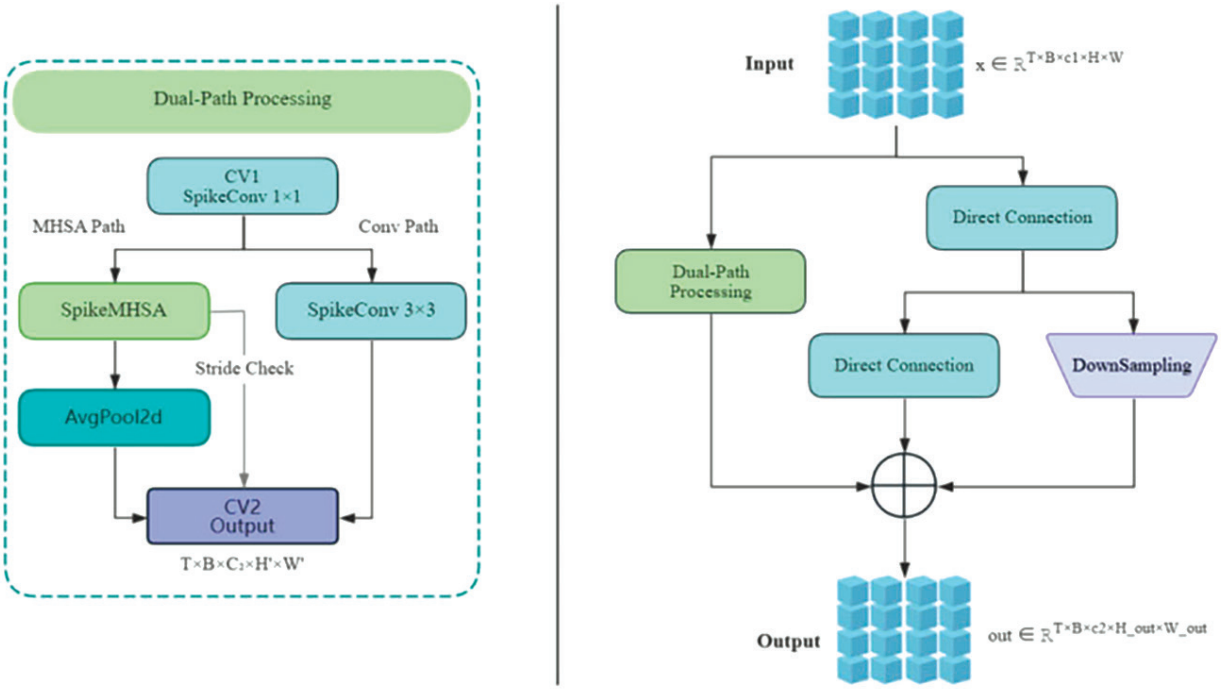

Fig. 3. Structure of SpikeBottleneckTransformer

2.3. SpikeBoT3 adapts the BoT3 module [8] to the spike domain. Whereas BoT3 couples Transformer-style global context with convolutional local detail, SpikeBoT3 replaces every operation with spiking equivalents – SpikeConv, SpikeBottleneckTransformer, and LIF neurons – cutting energy cost while keeping the multi-scale fusion intact (Fig. 4).

Its dual-branch layout runs in parallel. The main branch stacks SpikeConv, cascaded SpikeBottleneckTransformer blocks, and LIF neurons to build deep, globally aware features. The shortcut branch feeds the raw input through a shallow SpikeConv and LIF to preserve low-level detail. The two streams are concatenated channel-wise, fused by a final SpikeConv and LIF, and output as a spike train that carries both fine-grained and semantic information for the detection head.

2.4. SpikeSEAttention reworks SEAttention [9] for the spike domain. The original mechanism depends on floating-point GAP, fully-connected layers, and ReLU – operations ill-suited to binary, event-driven SNNs. We instead apply temporal average pooling to obtain channel-wise firing rates, keep the sigmoid for weight generation, and route the result through an LIF neuron to restore spike output. The pipeline thus stays fully sparse and end-to-end spiking (Fig. 5).

Specifically, SpikeSEAttention first receives a 5D spike sequence input:

$$X = \{x^{(t)}\}_{t=1}^{T} \in \{0,1\}^{T\times B\times C\times H\times W},$$

$$1\overline{x} = \frac{1}{T}\sum\nolimits_{t=1}^{T} x^{(t)} \in R^{B\times C\times H\times W}.$$

This feature map encodes the temporal information of the spike train as continuous values. Subsequently, Global Average Pooling (GAP) is applied per channel to compress the spatial information:

$$z_c = \frac{1}{HW}\sum\nolimits_{i=1}^{H} \sum\nolimits_{j=1}^{W} \overline{X}_c(i,j) \Rightarrow z = \mathrm{GAP}(\overline{x}) \in R^{B\times C}.$$

Yielding the channel descriptor z. Channel weights are then produced by a bottleneck fully-connected network without ReLU:

$$s = \sigma(W_2(W_1 z)) \in (0,1)^{B\times C},$$

where W_1, W_2 are learnable weights, and $\sigma(\cdot)$ is the sigmoid function. The computed static channel weights are broadcast across all time steps and multiplied element-wise with the original input:

$$\hat{x}^{(t)} = \hat{x}^{(t)} \otimes \tilde{s},\ \ \forall t = 1, ..., T,$$

where $\otimes$ denotes element-wise multiplication and $\tilde{s}$ denotes the weights shared across time. Finally, an LIF spiking neuron generates the output spike train:

$$y^{(t)} = \mathrm{LIF}(\hat{x}^{(t)}),\ \ \forall t.$$

The LIF activation ensures the output remains a discrete spike sequence [T, B, C, H, W], allowing seamless connection to subsequent SNN layers.

SpikeSEAttention drops ReLU in favor of an LIF output, keeping the entire pipeline spike-compatible for neuromorphic deployment. Shared temporal weights reduce redundant operations, while the SE gate amplifies salient channels and dampens noise, yielding cleaner feature maps.

3. Experiments and Results Analysis.

3.1. Datasets. The RSOD dataset [10; 11], a specialized remote sensing object detection dataset released by Wuhan University in 2015, includes: 446 images containing 4,993 aircraft; 189 images containing 191 playgrounds; 176 images containing 180 overpasses; and 165 images containing 1,586 oil drums.

3.2. Experimental Setup and Evaluation Metrics. All experiments in this study were conducted under a uniform hardware and software environment to ensure the reliability of the results. The detailed configuration parameters are listed in Table 1. The number of training epochs was set to 300. Parameters not mentioned in this paper use the default values of the baseline SpikeYOLO model (Table 1).

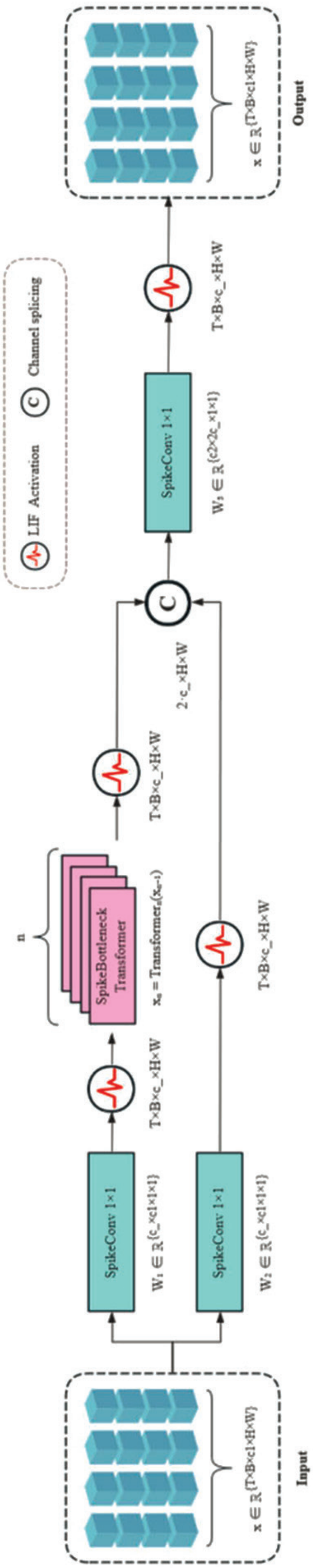

Fig. 4. Structure of SpikeBoT3

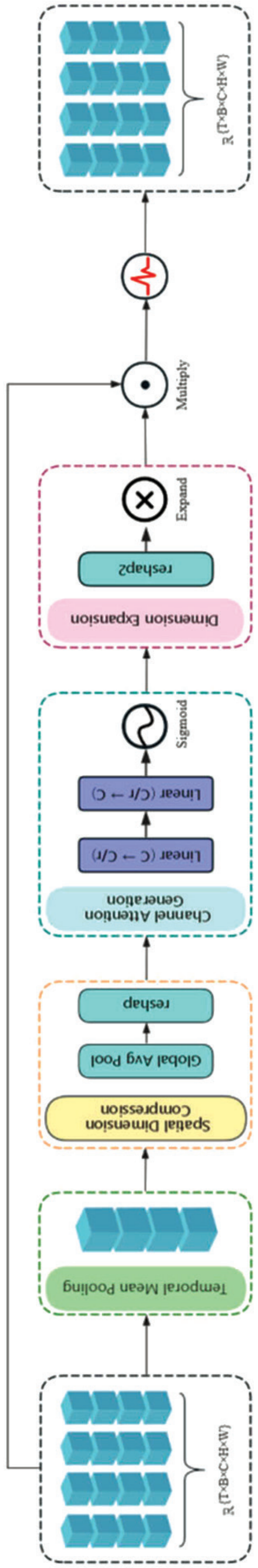

Fig. 5. Structure of SpikeSEAttention

Table 1. **Experimental Configuration**

Environment		Parameter	
Operating System	Ubuntu22.04	Learning Rate	0.01
GPU	RTX 4090(24GB) * 1	Iterations	300
Memory	120GB	Batch size	16
Python	Python 3.10 (Ubuntu22.04)	Workers	0
Framework	PyTorch 2.1.0	Image Input Size	640 × 640
Environment	CUDA 12.1	optimizer	auto

To comprehensively evaluate the performance of the proposed model, we employed Precision, Recall, Average Precision (AP), and mean Average Precision (mAP) as the primary evaluation metrics (Table 2).

Table 2. **Evaluation Metrics**

Symbol	Evaluation Indicators
AP	Average precision
P	Precision
R	Recall
IoU	Intersection over Union
mAP50	Average average precision (IoU = 0.5)
mAP 50–95	Average average precision (IoU = 0.5–0.95)

We evaluated the proposed method on the remote sensing datasets RSOD and NWPU VHR-10. For each model, we report the mean average precision at IoU = 0.5 (mAP@50), the average mAP over IoUs from 0.5 to 0.95 (mAP@50:95), and the energy consumption. Specifically, the power consumption formulas for ANN and SNN are as follows:

$$E_{\mathrm{ANN}} = O^2 \times C_{\mathrm{in}} \times C_{\mathrm{out}} \times K^2 \times E_{\mathrm{MAC}},$$

$$E_{\mathrm{SNN}} = (T \times D) f_r \times O^2 \times C_{\mathrm{in}} \times C_{\mathrm{out}} \times K^2 \times E_{\mathrm{AC}},$$

where O is the feature output size, C_{in} and C_{out} denotes the number of inputchannel and output channel, K is the kernel size, f_r denotes the average spikefiring rate, T is the timestep, D is the upper limit of integer activation during training. We follow the most commonly used energy consumption evaluation method in the SNN field [12]. All operations assume a 32-bit floating-point implementation on 45 nm technology, where EMAC = 4.6 pJ and EAC = 0.9 pJ [13].

3.3. Cross-Model Comparative Experiments. Under the same experimental conditions, we compared the proposed model with mainstream ANN detectors (YOLOv5n, YOLOv8n, YOLOv8m) and representative SNN detectors (EMS-YOLO, SpikeYOLO). The results are shown in Table 3.

Table 3. **Comparison Results**

Model	P (%)	R (%)	mAP50 (%)	mAP50–95 (%)
YOLOv5n	95.4	83.2	91.5	64.4
YOLOv8n	97.5	89.4	95.4	64.6
YOLOv8m	96.5	87.5	93.8	67.9
EMS-YOLO	89.8	88.2	91.8	59.4
SpikeYOLO	89.6	84.6	90.1	62.5
Ours	98.7	90.1	95.6	63.2

Against other SNNs, our model leads on every metric – up 8.9/1.9/3.8/3.8 points over EMS-YOLO and 9.1/5.5/5.5/0.7 over SpikeYOLO in P, R, mAP50 and mAP50-95. All prior SNNs fall below 90.0 % precision; out model achieves 98.7 % while holding 90.1 % recall, improving the balance between false alarms and missed targets.

Versus ANNs, we surpass YOLOv8n by 1.2/0.7/0.2 points and YOLOv8m by 2.2/2.6/1.8 in P, R and mAP50. On mAP50-95 our 63.2 % trails YOLOv8n (64.6 %) and YOLOv8m (67.9 %) – the stricter IoU threshold exposes the regression limits of discrete spike encoding – but we still lead SpikeYOLO by 0.7 points. Factoring in the event-driven power savings, the accuracy-efficiency balance favors our design.

Overall, we establish state-of-the-art performance among SNN detectors and outperform comparable ANNs on P, R and mAP50. Closing the high-IoU localization gap remains a direction for future work.

3.4. Quantitative Analysis of the Improved SpikeYOLO. The core advantage of SNNs lies in their low power consumption. To evaluate energy efficiency, we compared the proposed model with YOLOv8m and SpikeYOLO in terms of parameters, computational cost (GFLOPs), and per-inference energy consumption, as shown in Table 4. For SNN models, a time-step configuration of $T \times D = 4 \times 4$ is adopted, while the ANN model is treated as having $T \times D = 1$.

Table 4. **Energy consumption comparison**

Model	Parameters (M)	GFLOPs	$T \times D$	Power
YOLOv8m	25.8	78.7	1	181.01 mJ
SpikeYOLO	13.2	78.1	4 × 4	11.63 mJ
Ours	13.7	78.4	4 × 4	11.64 mJ

The three models have comparable computational costs (78.1–78.7 GFLOPs). However, the proposed model consumes only 11.64 mJ, which is about 1/15.6 of YOLOv8m (181.01 mJ), corresponding to a 93.6 % reduction in energy. The parameter count also drops from 25.8 to 13.7 M, a decrease of 46.9 %. This indicates that the energy efficiency gain does not come from reduced computation, but rather from SNNs replacing the floating-point multiply-accumulate (MAC) operations in ANNs with sparse spike-based accumulate (AC) operations. This event-driven property makes SNNs particularly suitable for edge devices and neuromorphic hardware.

3.5. Ablation Experiments. To analyze the actual effects of each module, we conducted ablation experiments on the RSOD dataset using SpikeYOLO as the baseline, with results presented in Table 5.

Table 5. **Ablation experiments**

SpikeYOLO	SpikeSEAttention	SpikeBoT3	P	R	mAP50	mAP50–95
√			89.6	84.6	90.1	62.5
√		√	93	90	94.3	65.3
√	√		95.2	88.2	92.7	63.7
√	√	√	98.7	90.1	95.6	63.2

Adding SpikeBoT3 alone lifted recall from 84.6 to 90.0 % and mAP50-95 from 62.5 to 65.3 %. The gain comes from long-range dependency modeling: the model now defects difficult targets by leveraging surrounding context, and the self-attention branch handles scale variations better. SpikeSEAttention alone increased precision from 89.6 to 95.2 % and mAP50 from 90.1 to 92.7 %, with mAP50-95 reaching 63.7 %. Channel reweighting sharpens spike-feature discrimination, reducing false positives while reaching salient channels across scales. Using both modules together, precision peaked at 98.7 % and mAP50 reached 95.6 %. The two mechanisms complement each other: SpikeSEAttention filters out spurious detections while SpikeBoT3 keeps recall high, yielding the best overall trade-off.

4. Conclusion. This research focuses on the central challenge in remote sensing object detection, namely, the difficulty of balancing high accuracy and low energy consumption. To address the issues of traditional convolutional neural networks (CNNs), including high energy consumption and challehging deployment on edge remote sensing platforms, this paper proposes an approach based on spiking neural networks (SNNs). Targeting the bottlenecks of SNNs in complex remote sensing scenarios – insufficient adaptability to multi-scale targets, dense small targets and omplex backgrounds, as well as weak capability for modeling long-range dependencies – a SpikeYOLO-Boost algorithm framework dedicated to remote sensing detection tasks is proposed. The framework is augmented with two novel components: the SpikeBoT3 hybrid spiking backbone for enhanced global context modeling, and the SpikeSEAttention spiking channel attention mechanism for robust multi-scale feature fusion. Evaluations on the RSOD dataset show that SpikeYOLO-Boost achieves significant improvements over the baseline. Ablation experiments confirm the synergistic efficacy of both modules in improving precision, recall, and feature representation. In summary, SpikeYOLO-Boost bridges the performance gap between SNN-based and mainstream ANN detectors. It provides a novel efficient solution for SNNs to perform complex object detection tasks on resource-constrained edge remote sensing platforms, such as on-orbit satellites and unmanned aerial vehicles (UAVs), and extends the application scope of spiking neural networks (SNNs) in the field of high-performance robust visual perception. Future work will focus on implementing of neuromorphic hardware and exploring its application in multimodal remote sensing analysis.

References

1. Wang Z., Fang Q., Han D. Research progress of on-orbit intelligent processing technology for imaging satellites. *Journal of Astronautics*, 2022, vol. 43, no. 3, pp. 259–270 (in Chinese). https://doi.org/10.3873/j.issn.1000-1328.2022.03.001

2. Cheng L., Liu X., Li L., Jiao L., Tang X. Deep adaptive proposal network for object detection in optical remote sensing images. *arXiv*, 2018. https://doi.org/10.48550/arXiv.1807.07327

3. Li Y., Wang M., Hwang K., Li Z., Ji T. LEO satellite constellation for global-scale remote sensing with on-orbit cloud AI computing. *IEEE Journal of Selected Topics in Applied Earth Observations and Remote Sensing*, 2023, vol. 16, pp. 9369–9381. https://doi.org/10.1109/JSTARS.2023.3316298

4. Cai C., Zhu Y., Sheng M., Li J., Shi Y., Zhou D., Xie Z., Zhang C. 3C resources joint allocation for time-deterministic remote sensing image backhaul in the space-ground integrated network. *arXiv*, 2025. https://doi.org/10.48550/arXiv.2510.09409

5. Luo X., Yao M., Chou Y., Xu B., Li G. Integer-valued training and spike-driven inference spiking neural network for high-performance and energy-efficient object detection. *arXiv*, 2025. https://doi.org/10.48550/arXiv.2407.20708

6. Xiao Y., Yuan Q., Jiang K., Huang W., Zhang Q., Zheng T., Lin C.-W., Zhang L. Spiking meets attention: Efficient remote sensing image super-resolution with attention spiking neural networks. *arXiv*, 2025. https://doi.org/10.48550/arXiv.2503.04223

7. Vaswani A., Shazeer N., Parmar N., Uszkoreit J., Jones L., Gomez A. N., Kaiser Ł., Polosukhin I. Attention is all you need. *arXiv*, 2023. https://doi.org/10.48550/arXiv.1706.03762

8. Srinivas A., Lin T.-Y., Parmar N., Shlens J., Abbeel P., Vaswani A. Bottleneck transformers for visual recognition. *arXiv*, 2021. https://doi.org/10.48550/arXiv.2101.11605

9. Hu J., Shen L., Albanie S., Sun G., Wu E. Squeeze-and-Excitation networks. *arXiv*, 2019. https://doi.org/10.48550/arXiv.1709.01507

10. Long Y., Gong Y., Xiao Z., Liu Q. Accurate object localization in remote sensing images based on convolutional neural networks. *IEEE Transactions on Geoscience and Remote Sensing*, 2017, vol. 55, no. 5, pp. 2486–2498. https://doi.org/10.1109/TGRS.2016.2645610

11. Xiao Z., Liu Q., Tang G., Zhai X. Elliptic Fourier transformation-based histograms of oriented gradients for rotationally invariant object detection in remote-sensing images. *International Journal of Remote Sensing*, 2015, vol. 36, no. 2, pp. 618–644. https://doi.org/10.1080/01431161.2014.999881

12. Panda P., Aketi S. A., Roy K. Toward scalable, efficient, and accurate deep spiking neural networks with backward residual connections, stochastic softmax, and hybridization. *Frontiers in Neuroscience*, 2020, vol. 14, art. 653. https://doi.org/10.3389/fnins.2020.00653

13. Horowitz M. 1.1 computing's energy problem (and what we can do about it). *IEEE International Solid-State Circuits Conference Digest of Technical Papers (ISSCC)*, San Francisco, 2014, pp. 10–14. https://doi.org/10.1109/isscc.2014.6757323

Information about the authors

Xianyi Wu – Postgraduate Student. E-mail: tigerv5872@gmail.com. ORCID: 0009-0003-6976-5386.

Guoyan Wang – Ph. D., Lecturer. E-mail: wangguoyan@nudt.edu.cn. ORCID: 0009-0006-2355-047X.

Ablameyko Sergey V. – Academician, D. Sc. (Physics and Mathematics), Professor. E-mail: ablameyko@bsu.by. ORCID: 0000-0001-9404-1206.

BingYan Liu – Ph. D. E-mail: 1iuby1349@gmail.com. ORCID: 0009-0004-4320-5214.

Информация об авторах

Xianyi Wu – аспирант. E-mail: tigerv5872@gmail.com. ORCID: 0009-0003-6976-5386.

Guoyan Wang – кандидат наук, преподаватель. E-mail: wangguoyan@nudt.edu.cn. ORCID: 0009-0006-2355-047X.

Абламейко Сергей В. – академик, д-р физ.-мат. наук, профессор. E-mail: ablameyko@bsu.by. ORCID: 0000-0001-9404-1206.

BingYan Liu – кандидат наук. E-mail: 1iuby1349@gmail.com. ORCID: 0009-0004-4320-5214.